AD-A103 075 GEORGIA INST OF TECH ATLANTA CENTER FOR THE ADVANCEM--ETC F/G 20/11
AN EVALUATION OF SEVERAL MOVING SINGULARITY FINITE ELEMENT MODE--ETC(U)
JUL 81 T NISHIOKA, R B STONESIFER, S N ATLURI N00014-78-C-0636
UNCLASSIFIED GIT-CACM-SNA-13 NL

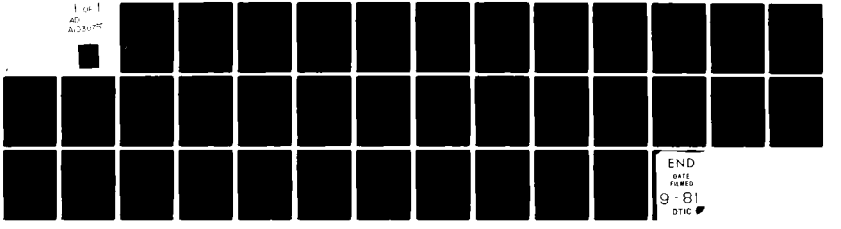

END
DATE FILMED
9-81
DTIC

Office of Naval Research

Contract N00014-78-C-0636 NR 064-610

Technical Report No. 15

Report No. GIT-CACM-SNA-13

by

T. Nishioka, R.B. Stonesifer and S.N. Atluri

July 1981

An Evaluation of Several Moving Singularity Finite Element Models for Fast Fracture Analysis.

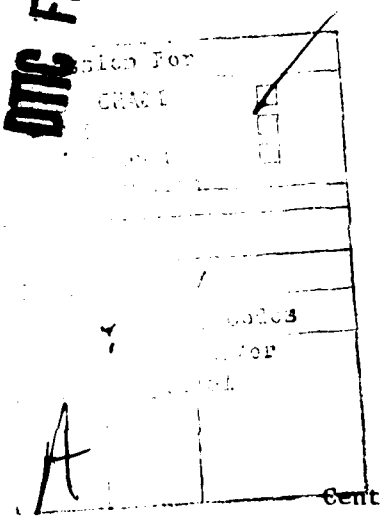

Center for the Advancement of Computational Mechanics
School of Civil Engineering
Georgia Institute of Technology
Atlanta, Georgia 30332

AN EVALUATION OF SEVERAL MOVING SINGULARITY FINITE ELEMENT MODELS FOR FAST FRACTURE ANALYSIS †

by

T. Nishioka*, R.B. Stonesifer**, S.N. Atluri***

Center for the Advancement of Computational Mechanics
School of Civil Engineering
Georgia Institute of Technology
Atlanta, Georgia 30332

*Research Scientist, **Graduate Student, *** Regents' Professor of Mechanics
†Based in Part on a presentation made at 2nd International Conference on Numerical Methods in Fracture Mechanics, Swansea, July 1980.

INTRODUCTION

In Refs. [1,2,3] the authors have presented a "moving singular-element" procedure for the dynamic analysis of fast crack-propagation in finite bodies. In this procedure, a singular-element, within which a large number of analytical eigen-functions corresponding to a steadily propagating crack are used as basis functions for displacements, may move by an arbitrary amount $\Delta\Sigma$ in each time-increment Δt of the numerical time-integration procedure. The moving singular element, within which the crack-tip always has a fixed location, retains its shape at all times, but the mesh of "regular" (isoparametric) finite elements, surrounding the moving singular element, deforms accordingly. An energy-consistent variational statement was developed in [1,2] as a basis for the above "moving singularity-element" method of fast fracture analysis. It has been demonstrated in [1,2] that the above procedure leads to a <u>direct evaluation</u> of the dynamic K-factor (s), in as much as they are unknown parameters in the assumed basis functions for the singular-element.

Solutions to a variety of problems, were obtained by using the above procedure and were discussed in detail in [1,3]. These problems included, among others: (*i*)constant-velocity, self-similar propagation of a finite central crack in a finite panel [analogous to the well-known Broberg's problem] (*ii*) stress-wave loading of a stationary central crack in a finite panel [analogous to the well-known problems of Baker; Sih et al; and Thau et al], (*iii*) constant-velocity propagation of a central crack in a panel, wherein, the propagation starts at a finite time after stress-waves from the loaded edge reach the crack, and (*iv*) constant velocity propagation of an edge-crack in a finite panel, whose edges parallel to the crack are subjected to prescribed, time-independent, displacements in a direction normal to the crack-axis analogous to the well-known

problems of Nilsson [4]. In Ref. [5], the results of numerical simulation of experimentally measured crack-tip versus time history in a rectangular-double-cantilever-beam (RDCB), as reported by Kalthoff et al [6], were reported. Also, in Ref. [5], the authors' results for the computed dynamic K-factor for RDCB were compared with the experimental (caustics) results of [6], and the independent numerical results of Kobayashi, [7] who uses a node-release technique in fast fracture simulation.

In this paper, the authors wish first to clarify and comment upon several aspects of the model formulation which appear in their Refs. [1,2]. Second, the model's accuracy and efficiency are evaluated in terms of less sophisticated models. Finally, the practicality of the special singular element for predicting crack growth for a given crack growth criterion is illustrated. In addressing the second topic, attention is focused on: (*i*) the effect of using only the stationary-eigen functions (or the well-known Williams' solution) in the moving singular-element for dynamic crack propagation, and (*ii*) the use of isoparametric elements with mid-side nodes shifted so as to yield the appropriate ($r^{-\frac{1}{2}}$) singularity [8,9]. Finally, some recent results are presented which illustrate the facility of the propagation-eigen-function singular element for predicting crack propagation behavior based on K_{ID} versus crack propagation speed as a crack growth criterion.

The Variational Principle

Since the details of the formulation are presented in Refs. [1,2], only those portions of the formulation necessary to the present discussion will be included here. Further, for simplicity the rather general equations of Refs. [1,2] will be specialized to the case of Mode I crack growth in bodies subject to traction free crack surfaces, zero body force and with geometry/

applied loading such that the model can make use of symmetry about the crack plane. In Ref. [2], the principal of virtu l work proposed as the governing equation for crack propagation during the period $[t_1,t_2]$ in which the crack elongates by amount $\Delta\Sigma$ is given as:

$$0 = \int_{V_2} \left\{(\sigma^2_{ij}+\sigma^1_{ij})\delta\varepsilon^2_{ij} + \rho(\ddot{u}^2_i+\ddot{u}^1_i)\delta u^2_i\right\} dV$$
$$- \int_{S_{\sigma_2}} (\bar{T}^1_i+\bar{T}^2_i)\delta u^2_i dS - \int_{\Delta\Sigma} \sigma^1_{ij}\nu^1_j\delta u^2_i dS. \qquad (1)$$

The superscripts 1 and 2 refer to quantities at times t_1 and t_2 respectively. The integrals in order of appearance refer to the volume of the body at time t_2, the portion of the surface of the body at time t_2 subjected to prescribed tractions and the new crack surface created between times t_1 and t_2. Note that the variational quantities $\delta\varepsilon^2_{ij}$ and δu^2_i reflect the kinematic constraint at t_2 and therefore are arbitrary on $\Delta\Sigma$. Making use of the small strain displacement relation, the symmetry of σ_{ij}, and using the divergence theorem, the first term of the volume integral in (1) becomes:

$$\int_{V_2} (\sigma^2_{ij}+\sigma^1_{ij})\delta\varepsilon^2_{ij} dV = \int_{\partial V_2} (\sigma^2_{ij}\nu^2_j+\sigma^1_{ij}\nu^1_j)\delta u^2_i dS - \int_{V_2} (\sigma^2_{ij,j}+\sigma^1_{ij,j})\delta u^2_i dV \qquad (2)$$

where ∂V_2 is the boundary of V_2. Noting that (i) $\Delta\Sigma$ is part of ∂V_2 (resulting in the last term of (1) dropping out), (ii) that S_{σ_2} is a part of ∂V_2 and (iii) that δu^2_i is zero on any portion of ∂V_2 that has prescribed displacements, we have:

$$\int_{V_2} \left\{\sigma^2_{ij,j}-\rho\ddot{u}^2_i+\sigma^1_{ij,j}-\rho\ddot{u}^1_i\right\}\delta u^2_i dV$$
$$+ \int_{S_{\sigma_2}} \left\{\bar{T}^2_i-\sigma^2_{ij}\nu^2_j+\bar{T}^1_i-\sigma^1_{ij}\nu^1_j\right\}\delta u^2_i dS \qquad (3)$$
$$- \int_{\Delta\Sigma} \sigma^2_{ij}\nu^2_j\delta u^2_i dS = 0$$

Since δu_i^2 is arbitrary (3) leads to:

$$\sigma_{ij,j}^2 = \rho\ddot{u}_i^2 + \rho\ddot{u}_i^1 - \sigma_{ij,j}^1 \quad \text{in } V_2 \tag{4a}$$

$$\sigma_{ij}^2 \nu_j^2 = \bar{T}_i^2 + \bar{T}_i^1 - \sigma_{ij}^1 \nu_j^1 \quad \text{on } S_{\sigma_2} \tag{4b}$$

and $$\sigma_{ij}^2 \nu_j^2 = 0 \quad \text{on } \Delta\Sigma \tag{4c}$$

It is seen that (4c) is nothing other than the condition that the new crack surface be traction free. Equation (4b) stipulates that traction boundary conditions be satisfied on S_{σ_2} and (4a) is a statement of dynamic equilibrium within the body. If one assumes that $\sigma_{ij,j}^1 \equiv \rho\ddot{u}_1^1$ then (4a) reduces to the usual equilibrium equation at t_2 (ie, $\sigma_{ij,j}^2 = \rho\ddot{u}_i^2$). Then since $\sigma_{ij,j}^2 = \rho\ddot{u}_i^2$ it follows that the state at t_3 must also satisfy the usual equilibrium equation and so forth. Therefore, (4a) is equivalent to the standard expression for dynamic equilibrium when the assumption that $\sigma_{ij,j}^1 \equiv \rho\ddot{u}_i^1$ is valid. A similar argument leads to (4b) reducing to the usual condition for satisfaction of traction boundary conditions.

In the finite element model formulation, the above assumption is not valid and therefore, the equations (4) do not reduce to those usually found in finite element model derivations. One reason for $\sigma_{ij}^1 \neq \rho\ddot{u}_i^1$ is that in modeling crack growth, it becomes necessary in the procedure of Refs. [1,2] to change the mesh configuration at each crack growth time step and to interpolate displacement, velocity and acceleration data at the new node locations. This interpolation will in general result in some disequilibrium in the interpolated solution. If, for example, we assume some disequilibrium at t_1 such that $\rho\ddot{u}_i^1 - \sigma_{ij,j}^1 = f$, then satisfaction of (4a) leads to $\rho\ddot{u}_i^2 - \sigma_{ij,j}^2 = -f$. Clearly, the disequilibrium at subsequent steps will be the same form (f) with the sign alternating at each step. Therefore, it would appear that the formulation of Ref. [1,2] should result in oscillations.

Numerical experimentation with the formulation has indeed shown this oscillation to occur. However, when used with the special singular element of Refs. [1,2] the only time it has occured at discernable levels is in static analyses. In dynamic analyses, it has been found that the inertial forces are generally large enough to make the oscillatory forces negligible.

Similar oscillation has been observed when implementing the proposed principle of virtual work with eight-noded isoparametric elements. (Wherein the appropriate crack tip singularity was obtained by shifting midside nodes as suggested by Ref. [8,9]). It is generally found that the oscillations when using the isoparametric elements are larger than those observed with the special singular element. This is believed to be the result of inherently larger interpolation induced disequilibrium with these less sophisticated elements.

A related variational principle for quasi-static crack growth in elastic-plastic bodies was also presented in [1]. To account for effects of history dependent plasticity and finite deformation gradients, an updated Lagrangean rate formulation was used. As a result of the formulation yielding an incremental analysis (as opposed to the computation of total state quantitites as in the elasto-dynamic analysis above), the effect of state quantities at t_1 appearing in the finite element equations for the solution at t_2 is fundamentally different. The variational statement, simplified for the case of zero body force, traction free crack surfaces and symmetrical modeling of Mode I crack growth, is given as:

$$\int_{V_1} \left[\tau^1_{ij} \dot{g}^Q_{ij} + \dot{S}_{ij} \delta g^L_{ij} \right] dV - \int_{S_{\sigma 1}} \dot{\bar{T}}_i \delta \dot{u}_i \, dS + \int_{\Delta\Sigma} \tau^1_{ij} \nu^1_j \delta \dot{u}_i \, d\Sigma = 0 \qquad (5)$$

where τ^1_{ij} are the Cauchy stress components of the solution at t_1 in the

current reference configuration (t_1, V_1, Σ_1), $\dot{u}_i$ are the incremental displacements in going from the reference state to the final state $(t_2, V_2, \Sigma_1+\Delta\Sigma)$ $\dot{\bar{T}}_i$ are the applied incremental tractions, $\dot{g}^Q_{ij}=\dot{u}_{K,i}\dot{u}_{K,j}$, $\dot{g}^L_{ij}=\dot{u}_{i,j}+\dot{u}_{j,i}$ and $\dot{S}_{ij}$ are the incremental second Piola-Kirchhoff stress components (or what are also known as Truesdell stress increments). Equation (5), through the use of the divergence theorem, leads to the following Euler-Lagrange equations:

$$(\tau^1_{kj}\dot{u}_{i,k})_{,j} + \dot{S}_{ij,j} + \dot{\bar{F}}_i = 0 \quad \text{in } V_1 \tag{6a}$$

$$(\tau^1_{kj}\dot{u}_{i,k}+\dot{S}_{ij})\nu_j - \dot{\bar{T}}_i = 0 \quad \text{on } S_{\sigma_1} \tag{6b}$$

$$(\tau^1_{kj}\dot{u}_{i,k}+\dot{S}_{ij}+\tau^1_{ij})\nu^1_j = 0 \quad \text{on } \Delta\Sigma \tag{6c}$$

Equation (6a) is the usual translational equilibrium condition associated with updated-Lagrangean formulations in terms of the second Piola-Kirchhoff stress and does not contain any additional terms such as found in equation (4a). Equation (6b) is the usual condition for satisfaction of traction boundary conditions and equation (6c) is the condition that the newly created crack surface be traction free. Further study of the derivation of equations (5) and (6) shows that there is nothing inherent in the formulation to account for (or correct) the error from interpolation of quantities from the finite element mesh at t_1 with crack length Σ_1 to the finite element mesh at t_1 with crack length $\Sigma_1+\Delta\Sigma$. However, the accumulated error at increment P (ε_p) can be measured by:

$$\varepsilon_P = \int_{V^P} \tau^P_{ij}\delta\dot{g}^L_{ij}dV - \int_{S^P_\sigma} \bar{T}^P_i\delta\dot{u}_i dS$$

which is a check on the equilibrium at increment p. Since this rate formulation does not result in terms which lead to oscillation of the solution it seems that formulation of the linear-elastic dynamic problem in terms of an incremental model similar to that for the elastic-plastic large deformation problem

would eliminate the trouble with oscillations while at the same time retain the crack growth modeling features.

Results of analyses which are presented later in this paper are largely based on the formulation as originally proposed in Ref. [1,2] since it appears that no significant change would result from a reformulation. The one exception to this are the results obtained through the use of isoparametric elements with midside nodes shifted so as give a singularity at the crack tip. In those analyses, the usual statement of virtual work is applied:

$$0 = \int_{V_2} \left\{ \sigma_{ij}^2 \delta\varepsilon_{ij}^2 + \rho \ddot{u}_i^2 \delta u_i^2 \right\} dV - \int_{S_{\sigma_2}} \bar{T}_i^2 \delta u_i^2 \, dS$$

Traction free crack surfaces are approximated by letting nodal forces on the crack surfaces be zero.

Singular Element for Dynamic Crack Propagation

A singular crack tip element was also developed in [1,2] and used in conjunction with the formulation (2) for the analysis of Mode I dynamic crack propagation in linear elastic two dimensional bodies. This singular element uses an arbitrary number of the displacement eigen-functions which come from the solution of a crack in an infinite body. For dynamic crack propagation, these eigen-functions are taken as those for the corresponding steady-state dynamically propagating crack in an infinite body. Equations (7) give the form for the assumed displacement, velocity and acceleration within the singular element:

$$\underset{\sim}{u}^s(\xi, x_2, t) = \underset{\sim}{U}(\xi, x_2, v)\underset{\sim}{\beta}(t) \tag{7a}$$

$$\dot{\underset{\sim}{u}}^s = \underset{\sim}{U}\dot{\underset{\sim}{\beta}} - v(\underset{\sim}{U})_{,\xi}\underset{\sim}{\beta} \tag{7b}$$

$$\ddot{\underset{\sim}{u}}^s = \underset{\sim}{U}\ddot{\underset{\sim}{\beta}} - 2v(\underset{\sim}{U})_{,\xi}\dot{\underset{\sim}{\beta}} + v^2(\underset{\sim}{U})_{,\xi\xi}\underset{\sim}{\beta} \tag{7c}$$

where $\underset{\sim}{U}$ is the matrix of eigen-functions (plus appropriate rigid body

modes), $\underline{\beta}$ is the vector of undetermined coefficients, v is the crack propagation speed and $(x_1 x_2)$ are the coordinates relative to the moving crack tip ($\xi = x_1 - vt$). It should be noted that (7b) and (7c) are obtained form (7a) through differentiation with respect to time with the assumption that <u>v is not a function of time</u>. The following comments should remove any incorrect notions that this in any way limits the use of the element to constant speed crack propagation. First, it has been shown [12] that the near-tip fields are the same for steady-state and transient crack propagation. Therefore, provided v at each time step reflects the current speed, there is no question that the eigen-functions for the element are correct and that the coefficient of the singular eigen-function (β_1) is indeed the Mode I stress intensity factor. A second consideration is that the associated stress eigen-functions do not satisfy the stress equilibrium-equation for non-steady-state (as viewed by an observer moving with the crack-tip).

$$\sigma_{ij,j} = \rho \left(\frac{\partial^2 u_i}{\partial t^2} - 2v \frac{\partial^2 u_i}{\partial \xi \partial t} + v^2 \frac{\partial^2 u_i}{\partial \xi^2} \right) \tag{8}$$

but instead, satisfy the corresponding steady equation:

$$\sigma_{ij,j} = \rho v^2 \frac{\partial^2 u_i}{\partial \xi^2} \tag{9}$$

While it would be preferred that equation (8) be satisfied exactly, the displacement finite element method does not require this. The stress equilibrium of (8) is satisfied in the usual approximate sense associated with the finite element method.

One common difficulty which arises when using more than one element type in a model is the lack of compatibility at the interface of the dissimilar elements. In Ref. [1,2] a method is explained for maintaining compatibility at the boundaries of the singular element which are shared by eight-noded isopara-

metric elements. This method involves selecting $\underset{\sim}{\beta}$ such that the following three error functionals are minimized:

$$I_1 = \int_{\rho_s} (\underset{\sim}{u}^s - \underset{\sim}{u}^R)^2 d\rho; \quad I_2 = \int_{\rho_s} (\dot{\underset{\sim}{u}}^s - \dot{\underset{\sim}{u}}^R)^2 d\rho; \quad I_3 = \int_{\rho_s} (\ddot{\underset{\sim}{u}}^s - \ddot{\underset{\sim}{u}}^R)^2 d\rho \qquad (10)$$

where $u^s, \dot{u}^s, \ddot{u}^s$ are as in equations (7), $u^R, \dot{u}^R \ddot{u}^R$ are displacements, velocities, and accelerations at the boundary of the eight-noded isoparametric elements, and ρ_s is the boundary of the singular element shared by isoparametric elements. This procedure gives $\underset{\sim}{\beta}$, $\dot{\underset{\sim}{\beta}}$ and $\ddot{\underset{\sim}{\beta}}$ in terms of $\underset{\sim}{q}_s$, $\dot{\underset{\sim}{q}}_s$ and $\ddot{\underset{\sim}{q}}_s$, the nodal displacements, velocities and accelerations of nodes on the boundary shared by the singular element and the isoparametric elements. In particular, $\underset{\sim}{\beta}$ is related to $\underset{\sim}{q}_s$ by

$$\underset{\sim}{\beta} = \underset{\approx}{A}\, \underset{\sim}{q}_s \qquad (11)$$

where $\underset{\approx}{A}$ is in general, a rectangular MxN matrix (M being the dimension of $\underset{\sim}{\beta}$ and N the dimension of $\underset{\sim}{q}_s$). The exact form of $\underset{\approx}{A}$ does not enter the present discussion but can be found in [1,2]. The question to be addressed here concerns the constraints which must be placed on the dimension of $\underset{\approx}{A}$ (and therefore $\underset{\sim}{\beta}$). It is well known that in hybrid finite elements there is a restriction on the number of internal parameters ($\underset{\sim}{\beta}$) so that the matrix equations relating these parameters to the unknowns of the final finite element equations are non-singular [11]. It should be noted that the current procedure is not (strictly speaking) a hybrid procedure and therefore the matrix $\underset{\approx}{A}$ relating $\underset{\sim}{\beta}$ to $\underset{\sim}{q}_s$ does not pose the same problem. However, the following does show there is a restriction on the dimension of $\underset{\sim}{\beta}$. In the derivation of [1,2] there are nine nodal points and therefore eighteen degrees of freedom associated with the singular element. All of these are on its boundary (denoted ρ_s in (10)) as illustrated in the typical mesh of Figure 1. To ascertain the behavior of the singular element with differing numbers of eigen-functions (ie, differing dimensions

for $\underset{\sim}{\beta}$) the eigen-values and eigen-modes of the singular element for zero crack speed were calculated. In making the calculations, the symmetry plane nodal displacement normal to the crack plane was constrained since no eigen-functions were included for rigid body translation normal to the crack plane. Based on the deletion of this one degree of freedom it can be seen that the singular element must have seventeen deformation modes (eigen vectors) and should have only one zero energy mode (eigen value of zero), corresponding to a rigid body translation. In varying the dimension of $\underset{\sim}{\beta}$ (call it M) it was found that for M = 17, there was one zero eigenvalue which through examination of the eigenvector did indeed correspond to the desired rigid body translation parallel to the crack plane. When cases for $M < 17$ were considered, the number of these zero energy modes (P) was $P = 18-M, (M \leq 17)$. These excess zero energy modes are clearly undesirable. It was also observed that the desired rigid body mode was no longer present when these extra modes occured. The constraint on M for the current configuration is therefore $M \geq 17$. In the general 2D case where N is the number of unconstrained nodal degrees of freedom associated with the singular element we must have $M \geq N$, where M includes the appropriate number of special rigid body displacement functions. If we denote the number of these rigid body functions by R, then the required number of crack solution eigen-functions (C) is given by $C \geq N-R$ which is exactly that constraint found for the number of assumed element stress functions in hybrid stress finite element models [11]. The results presented in [1, 3, 5] and to be presented here have used M=20 therefore satisfying the above constraint.

Procedures for Simulation of Crack Growth

The modeling of crack propagation with either the special singular element

or with the singular isoparametric elements requires the finite element mesh in the region of the crack tip to be modified at each time step for which crack growth occurs. The procedure used here (and in [1,3,5] is to shift the singular element (s) without distortion, (as shown in Figure 2) so that it is only the regular elements surrounding the special modeling region which become distorted. An important point which differentiates this procedure from the more common node release techniques for crack growth is that the size of the increment of crack growth ($\Delta\Sigma$) is not restricted by nodal spacing but rather can be made as small as desired. Figure 2 also illustrates that the distortion of elements periodically reaches a critical degree at which time the crack tip region of the model is remeshed before applying the shifting procedure. Since this procedure involves the shifting of nodal points and since the nodal quantities of displacement, velocity and acceleration at each time step appear in the difference equations associated with the Newmark time integration scheme for the solution at the subsequent time step, it is necessary to use interpolation procedures to obtain correct values for the shifted nodes.

Considerations of Efficiency and Accuracy

In the previous sections, the discussion was largely in terms of particular features of the variational principle or singular element derivation. Here the discussion will be of a broader nature with most of the attention being focused on the more general attributes of efficiency and accuracy.

The singular element with crack propagation speed dependent eigen-functions has several attractive features which stem directly from the use of the analytical solution for the near-crack-tip field. First, the traction free crack surface conditions are satisfied exactly. Second, the coefficient of the

singular eigen-function is the Mode I stress intensity factor and is obtained directly without recourse to indirect energy based procedures or extrapolation methods. Third, because many eigen-functions are used, the accuracy of the solution is less sensitive to the singular element size than for elements with less elegant basis functions.

As might be expected, this element also has some features which tend to offset the above positive ones. One such feature is that the propagation-eigen-functions lead to a non-symmetric stiffness matrix. However, since the non-symmetry is localized to rows and columns corresponding to q_s, the additional effort in solving the equations is not excessive. Another aspect of using special elements which requires attention is the inherent incompatibility of displacement with neighboring elements. The procedure proposed in [1,2] and used here involves satisfying compatibility along ρ_s in an integrated least square sense as shown in equation (10).

In order to weigh the above positive features against the negative, two alternative models are considered. The first alternative is to use a similar special singular element but to substitute stationary crack eigen-functions for the propagating crack eigen-functions. This substitution has two effects. First, the stiffness matrix becomes symmetric. Second, the coefficient of the singular eigen-function can no longer be interpreted as K_I, the Mode I stress intensity factor. At first, this loss seems a dear price to pay since it would appear that one must resort to indirect procedures for determining K_I such as energy calculations or the fitting of propagation-eigen-functions to the near field solution! However, K_I can be obtained directly from the stationary-eigen-function element solution using a simple formula described later. With this question of calculating K_I answered, it remains to be seen how well the chosen number of stationary functions (twenty) can accomodate the distored

near field displacement patterns of a propagating crack.

It is clear that whether one uses stationary-eigen-functions or propagation-eigen-functions, the special element will still require additional work to ensure compatibility with neighboring elements. To ascertain the benefits of eliminating this additional work, a third model is considered. This model, as mentioned previously, uses eight-noded isoparametric elements exclusively. The $r^{-\frac{1}{2}}$ singularity in stress and strain is incorporated in the model by shifting midside nodes on element edges joining the crack tip node to the quarter-point of the element side as illustrated in Figure 1. To ensure the correct behavior in all angular directions from the crack tip, the elements adjoining the crack were degenerated to the triangular form seen in Figure 1. While this model has no problem in terms of compatibility, it does have a problem in terms of calculation of K_I. One has virtually no choice but to resort to energy methods, fitting of eigen-functions or extrapolation procedures. Since a major consideration in comparing the above models is the accuracy and ease of computing K_I, the indirect procedures for computing K_I with the stationary eigen-function model and quarter-point isoparametric element model will be described.

Indirect Methods for Computing K_I

As pointed out previously, when the propagation-eigen-function singular element is used, K_I is evaluated directly during the solution procedure and therefore indirect methods for evaluation K_I are not required. However, that does not mean that these methods can not be used and in fact the comparison of K_I from alternate procedures is a good manner for checking the consistency of the solution.

The first two indirect procedures rely on the well known relationship between K_I and the fracture energy release rate (G) for pure Mode I fracture:

$$K_I = \sqrt{\frac{2\mu G}{f(\alpha_d,\alpha_s)}} \tag{12}$$

where $f(\alpha_d,\alpha_s) = \alpha_d(1-\alpha_s^2)/[4\alpha_d\alpha_s - (1+\alpha_s^2)^2]$

$\alpha_d^2 = 1 - (v/C_d)^2$; $\alpha_s^2 = 1 - (v/C_s)^2$

$C_s^2 = \mu/\rho$

$C_d^2 = \frac{2\mu}{\rho}\left(\frac{1-\nu}{1-2\nu}\right)$ for plane strain

or $C_d^2 = \frac{2\mu}{\rho}\left(\frac{1}{1-\nu}\right)$ for plane stress

In the above, v is the crack propagation speed, μ the shear modulus, ν the possons ratio, ρ the mass density, C_s the shear wave speed and C_d the dilatational wave speed. For the limiting case as ν goes to zero, we have

$$f(1,1) = 1-\nu \text{ for plane strain}$$

$$\text{or} \quad f(1,1) = \frac{1}{1+\nu} \text{ for plane stress} \tag{13}$$

To make use of (12), one must evaluate G. This has been done in the present work using three different approaches. The first approach to determining G is through an energy balance. This is done in crack propagation analysis most easily by considering the energy of the system at two adjacent time steps t_1 and t_2 between which an increment in crack length $\Delta\Sigma$ has occured ($\Delta\Sigma=\Sigma_2-\Sigma_1$). If we define the increment in work done on the system by the applied traction and displacement boundary conditions as $\Delta W = W_2-W_1$ and similarly denote the change in strain energy by ΔU and the change in kinetic energy by ΔT then an average G for the interval (t_1,t_2) is given by:

$$G = \frac{\Delta W - \Delta T - \Delta U}{b(\Delta\Sigma)} \tag{14}$$

where b is the length of the propagating crack front.

The second approach to computing G is to use a crack closure integral. This calculation involves the tractions on $\Delta\Sigma$ existing at t_1. For pure Mode I

fracture behavior one has only displacement component u_y and traction component T_y present at $\Delta\Sigma$. An average G for the interval t_1, t_2 is given by:

$$G = \frac{-1}{\Delta\Sigma} \int_{\Delta\Sigma} T_y(x,t_1)u_y(x,t_2)dx \tag{15}$$

where u_y is half the total crack opening due to the use of symmetry in the model. The factor of ½ usually observed in linear elastic work evaluations is canceled by a factor of 2 which accounts for the use of symmetry in the model.

The third method for evaluating G is the J-integral. It is well known that G=J for elastic bodies and therefore is obtained from the definition of J in the current symmetrical dynamic analysis of a Mode I crack [10]:

$$J=2 \left\{ \int_A \rho \ddot{u}_j \frac{\partial u_j}{\partial x} dA + \int_\Gamma \left(W n_x - T_j \frac{\partial u_j}{\partial x} \right) ds \right\} \tag{16}$$

where ρ is the mass density, W is the strain energy density, Γ is a curve connecting the upper crack surface to the symmetry plane ahead of the crack (which is propagating in the x coordinate direction), A is the two-dimensional region enclosed by Γ, n_x is the x-component of the outward unit normal to Γ and T_j is the traction vector acting on Γ (outward positive). The factor of 2 again reflects the use of symmetry in modeling.

In addition to the above energy related procedures, two additional methods are used here for determining K_I. The first of these two involves the fitting of near field displacements with the propagation-eigen-functions discussed previously. This method is quite general in nature and can be used with either the special stationary-eigen-function element or with the quarter-point singular elements. The procedure is to use equations (10) to obtain an equation of the form (11) such that the coefficient of the singular propagation-eigen-function

$\beta_1(\beta_1=K_I)$ can be related to the near field nodal displacements q_s.

The final procedure for obtaining K_I is primarily applicable to the stationary-eigen-function element and results in the evaluation of K_I from this element being nearly as direct as when using the propagation-eigen-function element. Let β_1^P be the undetermined coefficient of the singular propagation-eigen-function ($\beta_1^P=K_I$). Let β_1^S be the corresponding coefficient of the stationary-eigen-functions, noting $\beta_1^S = \beta_1^P = K_I$ only if v, the crack propagation speed, is zero. Using the definition of G for Mode I fracture:

$$G \triangleq \lim_{\Delta\Sigma\to 0} \frac{-1}{\Delta\Sigma} \int_0^{\Delta\Sigma} T_y(x)\, u_y(x-\Delta\Sigma)\, dx \tag{17}$$

it is possible to obtain two equivalent definitions of G in terms of β_1^P or β_1^S by substitution of the respective singular eigen-functions into (17):

$$G \triangleq \frac{f(\alpha_d,\alpha_s)}{2\mu} (\beta_1^P)^2 \text{ and } G \triangleq \frac{f(1,1)}{2\mu} (\beta_1^S)^2 \tag{18}$$

From (18) it is then seen that β_1^P which is always equal to K_I can be related to β_1^S by:

$$K_I = \beta_1^P = \sqrt{\frac{f(1,1)}{f(\alpha_d,\alpha_s)}}\, \beta_1^S \tag{19}$$

where $f(1,1)$ and $f(\alpha_d,\alpha_s)$ are as defined in the text immediately following equation (12).

Crack Propagation Computations for Comparison of Models

The primary purpose of these computations is to compare results using several levels of modeling sophistication. To keep the problem from obscuring the basic differences in modeling techniques, a rather simple combination of geometry and loading was selected. The problem which was considered previously in Ref. [3] is that of the constant velocity propagation of an edge crack in a square sheet whose edges

parallel to the direction of crack propagation are subjected to uniform displacements u_2 in the direction normal to that of crack propagation. The dimensions and mesh configuration are depicted in Figure 1. This problem is analogous to that treated by Nilsson [4] who obtained an analytical solution for steady-state stress-intensity factor for the constant velocity propagation of a semi-infinite crack in a finite-height, infinite-width strip. In the following, the material properties are ν=0.286, μ=2.94 x 10^4N/mm^2 and ρ=2.45 x 10^{-6}kg/mm^3. Three levels of constant crack velocity propagation, (v/C_s)=0.2,0.4,0.6 are considered. In each case, the initial crack length, (Σ_o/W) is 0.2. For each case, the crack growth increment size is maintained constant (as opposed to time step size) at a value of $\Delta\Sigma/W$=0.005 which corresponds to 2.5 percent of the singular element's dimension in the crack propagation direction.

In these analyses the uniform prescribed displacement is applied statically at t=0 sec. While maintaining this prescribed displacement, the crack is then made to propagate at a uniform speed. This procedure results in crack acceleration over the first time step and since the time step size is varied so as to maintain the crack growth increment size constant, this acceleration will also differ for each value of the uniform crack speed.

$\underline{v=0.2C_s}$ The computated $K_I(t)$ for this lowest considered propagation speed are illustrated in Figure 3. Note that the computed $K_I(t)$ are normalized with respect to K_s^∞, which is the static K_I for the infinite width strip problem of Nilsson (where $K_s^\infty=(\bar{u}_2E)/\sqrt{h}(1-\nu^2)$ and are plotted as a function of nondimensional crack length (Σ/W). In each of Figures 3,4 and 5 the arrows indicate the crack lengths at which the remeshing procedure (illustrated in Figure 2) takes place. The dashed lines of Figures 3, 4 and 5 indicate the steady-state value

of K_I for the infinite strip problem due to Nilsson [4]. The nearness to unity of the dashed line of Figure 3 indicates the relatively low velocity dependence of the strip solution at this crack speed.

The solid curve of Figure 3 represents the values of K_I from the propagation-eigen-function element and as discussed previously are determined directly as the coefficient of the singular eigen-function during the solution. The solid points of Figure 3 are the results from the stationary-eigen-function element. To illustrate the small effect of crack speed at $v=0.2C_s$, the plotted values are just the coefficient of the singular eigen-function but because of the non-zero crack speed are not strictly speaking values of K_I. To obtain correct values of K_I in this case, one would have to use equation (19). Since this correction would uniformly lower all these points by only 1.4%, these corrected values are not plotted. It can be seen, however, that this correction would indeed tend to improve the already excellent agreement with the propagation-eigen-function element.

The open sympols of Figure 3 are the results of the quarter-point isoparametric element computations. The open circular points are based on a G obtained through a global energy balance (14) which is then converted to K_I through equation (12). It can be seen that except for the first four time steps, these points agree quite well with the propagation-eigen-function element solution. The open triangular points are based on a G obtained through the crack closure integral of equation (15) and then converted to K_I through equation (12). It is

clear from Figure 3 that the crack closure integral procedure is inferior to the energy balance procedure when used with the isoparametric elements. This is attributed to the inherent inaccuracy of the boundary tractions for the isoparametric element which are required when using equation (15). It should be noted that a very satisfactory aspect of the crack growth modeling procedure used here is that none of the curves in Figure 3 show erratic behavior which can be related to the remeshing procedure. From Figure 3, it seems that any one of the three models is adequate for the problem when $v=0.2C_s$.

$\underline{v=0.4C_s}$ The results for this intermediate case are given in Figure 4. Again, the dashed curve represents the steady-state infinite strip solution. To illustrate the increasing effect of the crack speed on the crack tip field, the solid points are again the coefficient of the singular term of the stationary-eigen-function solution and must be modified via equation 19 before being interpretable as K_I. The solid square points are these modified values. It can be seen that the agreement between the propagation-eigen-function solution and the stationary eigen-function solution is still quite good despite the increased effect of crack speed on the crack tip field.

The quarter-point isoparametric element results are indicated by open circular points. Here again, the global energy balance procedure has been used. Unlike the results for $v=0.2C_s$, there is a pronounced difference between the isoparametric element results and the special element results. It is believed that this difference is largely due to the inadequacy of the four elements used here to model the increasingly contorted displacement and stress fields which occur with increasing crack speed. An increase in the number of triangular elements in the angular direction might be expected to remedy this deficiency. The inadequacy of the element refinement is further evidenced

by the noticeable disturbance in the K_I values accompanying each remeshing.

$\underline{v=0.6C_s}$ The results for this largest considered crack speed are presented in Figure 5. Here again the dashed line is the steady-state infinite strip solution and the solid curve the propagation-eigen-function solution. The solid square points are the K_I values from the stationary-eigen-function element solution, and are obtained from the β_1^s (solid circular points) using equation 19. The solid triangular points are also K_I values from the stationary-eigen-function solution but were obtained through fitting the near field nodal displacements (q_s) with the propagation-eigen-functions using the method described previously. Nineteen eigen-functions plus the one rigid body mode were used in this fitting procedure. Both of the above procedures for treating the stationary-eigen-function-solution yield results which agree quite well with the propagation-eigen-function-solution but clearly the one represented by equation 19 is preferred due to the ease of application.

The results from the quarter-point isoparametric elements are plotted in Figure 5 using open circular points. Unlike the results presented at $v=0.4C_s$ and $v=0.2C_s$, the values of K_I plotted here were obtained through the J-integral as defined by (16). Though the results based on the global energy balance procedure are not presented here, they were found to agree quite well with those using the J-integral except that there was substantially more "noise". This "noise" became particularly apparent at positions where remeshing was required.

From these calculations involving crack propagation speed ranging from $0.2C_s$ to $0.6C_s$, it appears that for these crack-speed ranges the propagation-eigen-function element has no significant advantages over the stationary-eigen-function element either in terms of accuracy or in terms of ease of computing K_I, other than being more theoretically consistent and appealing. Since there

is additional effort in dealing with the non-symmetric matrices which accompany the propagation-eigen-function formulation, it seems the stationary-eigen-function element might be more effectively implemented to obtain results within a tolerable engineering accuracy. The large number of eigen-functions used in these special element formulations in order to produce no spurious kinematic deformation modes is believed to be the reason for the high degree of accuracy attained with the stationary-eigen-function element in the analysis of fast crack propagation. It was observed that the use of four quarter-point isoparametric elements was quite adequate at $v=0.2C_s$, but that by $v=0.4C_s$ the accuracy had become marginal (5-10% difference from special element results). In considering the effect of crack speed on the isoparametric element solution accuracy, it should be kept in mind that experimentally measured crack speeds often fall below $0.3C_s$. If one needs to consider higher speeds, mesh refinement seems to be necessary.

Application to Prediction of Crack Growth

In the computations of [1,3,5] and in those of the previous section, the loading of the body and the crack growth history are used as input to the analysis. The output of each of these "generation phase" computations is K_I as a function of time, crack length or crack speed. The subject of this section are computations of a reverse nature. That is, the input to the computation is the loading of the body and a crack growth history. This type of analysis is referred to as an "application phase" computation.

One feature of the special eigen-function elements which has proved to be quite useful in the application type analysis is that in addition to K_I being computed directly from q_s one also has $\frac{\partial K_I}{\partial t}$ and $\frac{\partial^2 K_I}{\partial t^2}$ as a result of the minimization of the error functionals of equation (10).

Having these quantities at some time, say $t=t_1$, simplifies the prediction of crack velocity for the subsequent time step since the value of K_I can extrapolated using a Taylor series expansion. More precisely, in order to determine $\Delta\Sigma=\Sigma_2-\Sigma_1$ using a crack growth criterion based on K_I, one needs to have an average K_I for the interval (t_1,t_2). For the propagation-eigen-function element, this average K_I is predicted in terms of quantities at t_1 by:

$$K_{Ip} = \beta_1^p(t_1) + \frac{\Delta t}{2}\dot{\beta}_1^p(t_1) + \frac{(\Delta t)^2}{8}\ddot{\beta}_1^p(t_1) \qquad (21)$$

where $\dot{\beta}_1^p = \frac{\partial K_I}{\partial t}$ and $\ddot{\beta}_1^p = \frac{\partial^2 K_I}{\partial t^2}$. Having K_{Ip} one uses the criterion to obtain v which is then used to obtain $\Delta\Sigma = v\Delta t$. Having $\Delta\Sigma$ the finite element mesh for the crack length Σ_2 can be generated and the solution at t_2 obtained. It should be noted that a similar prediction procedure to (21) exists for the stationary eigen-function element. Through the differentiation of (19) with respect to time one can obtain:

$$K_{Ip} = \sqrt{\frac{f(1,1)}{f(\alpha_d,\alpha_s)}}\left[\beta_1^S(t_1) + \frac{\Delta t}{2}\dot{\beta}_1^S(t_1) + \frac{(\Delta t)^2}{8}\ddot{\beta}_1^S(t_1)\right] \qquad (22)$$

An application phase calculation for a double cantilever beam specimen, identical to specimen No. 4 of Kalthoff, et al [6], has been completed using the K_{ID} versus $\dot{\Sigma}$ relation shown in Figure 6 as a crack growth criterion. This curve and the crack initiation fracture toughness for the computation (K_{IQ} = 2.32 $MNm^{-3/2}$) are identical to the ones used by Kobayashi [7]. The predicted K_I vs t_1, Σ vs t and $\dot{\Sigma}$ (or v) vs t which were obtained using the propagation-eigen-function element are shown in Figure 7 along with the corresponding experimental results of Kalthoff, et al [6] and numerical results of Kobayashi [7]. The present plane stress analysis used $E=3380MN/m^2$, $\nu=0.33$ and $\rho=1172kg/m^3$.

It can be seen in Figure 7 that the $\dot{\Sigma}$ vs t results are virtually indistin-

guishable from the experimental results and that even the v vs t results agree quite well. In comparing the K_I curves it is seen that there is quite good agreement for approximately the first half of the total crack growth. At about midway, however, the computed K_I increases briefly while the experimental values drop. Before arrest occurs, there is again good agreement, however.

One possible explanation for the above disparity is that the Araldite B used by Kalthoff shows some rate dependence even though it was selected over similar materials because of its relatively low rate dependence [6]. For example, the dynamic elastic constants quoted in [6] are E=3660 and ν=0.39, whereas the static values, used in the analysis, are E=3380 MN/m^2 and ν=0.33. While this rate dependence must surely have some effect on the specimens response, it has been observed through numerical experiments that other aspects of the experimental procedure and numerical modeling procedure also have quite large effects. The results of these sensitivity studies are being presented in a companion paper [13].

CONCLUSION

The comparison of the propagation-eigen-function element, the stationary-eigen-function element, and the quarter-point isoparametric element in terms of accuracy and efficiency leads to several conclusions. The two eigen-function elements showed similar accuracy at all crack speeds up to $0.6C_s$ while the isoparametric element model started showing significant differences between $0.2C_s$ and $0.4C_s$. While the quarter-point isoparametric elements were the least expensive to use (2/3 the cost of the stationary-eigen-function element and 1/2 that of the propagation-eigen-function element) their sensitivity to crack speed and the need to use indirect methods to obtain K_I reduce their initial attractiveness. Furthermore, for application type

analyses the lack of $\dot{K}_I$ and $\ddot{K}_I$ may complicate the use of isoparametric type elements to the point that they lose their cost advantage. Another conclusion to be drawn from the comparison of the models is that the stationary-eigen-function element has all the attractive features of the propagation eigen-function element without the disadvantage of non-symmetric stiffness matrices. Also, because the matrices are not crack speed dependent, they do not need to be recomputed each time crack speed changes. Finally, the eigen-function elements seem particularly attractive for application phase analysis since at each time step one has not only K_I but also $\frac{\partial K_I}{\partial t}$ and $\frac{\partial^2 K_I}{\partial t^2}$; thus simplifying the prediction of crack behavior in the subsequent time step.

The application phase anlaysis of the double cantilever beam specimen illustrated the utility of the propagation-eigen-function element for predicting crack growth behavior using K_{ID} versus v as a crack growth criterion. Since the stationary-eigen-function element showed very good agreement with the propagation-eigen-function element in the generation type analyses and since the predictive logic for application type analyses is the same for both element types, it seems the stationary-eigen-function element is also well suited to application computations.

The propagation-eigen-function element, even if more expensive to use than the other two special elements discussed above, is nevertheless more consistent and appealing in terms of theoretical formulation, and application to basic research in dynamic crack propagation in finite bodies. Due to this reason, extensive dynamic fracture studies, of both 'generation' and 'application' type, on laboratory specimens such as the rectangular double cantilever beam (RDCB) tapered double cantilever beam (TDCB), and edge crack specimen, were conducted by the authors using the presently described propagation-eigen-function special

element.

These numerical results were compared with available experimental data. A detailed presentation of these results is made in a companion paper [13], in which the effects of specimen geometry, input crack-velocity history, and input dynamic fracture toughness property data, are discussed in detail.

ACKNOWLEDGEMENTS

This work was supported by the U.S.O.N.R. under contract No. N00014-78-7636. The authors are grateful to Dr. N. Perrone for his timely encouragement. The authors also thank Ms. M. Eiteman for her care in the preparation of this manuscript.

REFERENCES

[1] Atluri, S.N., Nishioka, T., and Nakagaki, M., "Numerical Modeling of Dynamic and Nonlinear Crack Propagation in Finite Bodies, by Moving Singular Elements" In Nonlinear and Dynamic Fracture Mechanics, Ed. N. Perrone, and S.N. Atluri AMD-Vol 35, ASME, NY, 1979, pp 37-66.

[2] Nishioka, T., and Atluri, S.N., "Numerical Modeling of Dynamic Crack Propagation in Finite Bodies, by Moving Singular Elements, Part I - Theory", Journal of Applied Mechanics, ASME, 1980 (In Press).

[3] Nishioka, T., and Atluri, S.N., "Numerical Modeling of Dynamic Crack Propagation in Finite Bodies, by Moving Singular Elements, Part II - Results" Journal of Applied Mechanics, ASME, 1980 (In Press).

[4] Nilsson, F., "Dynamic Stress-Intensity Factors for Finite Strip Problems", Int. Jnl. of Fracture, Vol., No. 4, 1972, pp 403-411.

[5] Nishioka, T., and Atluri, S.N., "Efficient Computational Techniques for the Analysis of Some Problems of Fracture in Pressure Vessel and Piping" to be presented at ASME Pressure Vessels and Piping Conference, San Francisco, Aug. 1980.

[6] Kalthoff, J.F., Beinert, J., Winkler, S., "Measurements of Dynamic Stress Intensity Factors for Fast Running and Arresting Cracks in Double-Cantilever-Beam Specimens", Fast Fracture and Crack Arrest, ASTM STP 627, G.T. Hahn and M.F. Kanninen, Eds. ASTM, 1977, pp 161-176.

[7] Kobayashi, A.S., "Dynamic Fracture Analysis By Dynamic Finite Element Method-Generation and Propagation Analyses", In Nonlinear and Dynamic Fracture Mechanics, Ed. N. Perrone, and S.N. Atluri, AMD-Vol 35, ASME, NY, 1979, pp 19-36.

[8] Henshell, R.D., Shaw, K.G., "Crack Tip Finite Elements are Unnecessary", Int. J. Num. Meth. Engng., Vol 9, 495-507, 1975.

[9] Barsoum, R.S., "On the Use of Isoparametric Finite Elements in Linear Fracture Mechanics", Int. J. Num. Meth. Engng., Vol 10, 25-37, 1976.

[10] Kishimoto, K., Aoki, S., Sakata, M., "Dynamic Stress Intensity Factors Using J-Integral and Finite Element Method", Engng. Fracture Mech., Vol 13, pp 387-394 (1980).

[11] Pian, T.H.H., Tong, P., "Basis of Finite Element Methods for Solid Continua", Int. J. Num. Meth. Engng., Vol 1, 3-28 (1969).

[12] Achenbach, J.D. and Bazant, Z.P., "Elastodynamic Near-Tip Stress and Displacement Fields for Rapidly Propagating Cracks in Orthotropic Materials", J. Appl. Mech., 42, p 183 (1975).

[13] Nishioka, T., Atluri, S.N., "Numerical Analysis of Dynamic Crack Propagation: Generation & Prediction Studies" submitted to Jnl. of Engineering Fracture Mechanics, 1980.

Figure 1. Finite element mesh for the numerical approximation to the infinite strip problem of Nilsson [4].

Figure 2. Illustration of the shifting/remeshing procedure for modeling crack growth.

Figure 3. Nondimensionalized K_I vs Σ for constant velocity crack propagation ($v=0.2C_s$) in the model of Figure 1.

Figure 4. Nondimensionalized K_I vs Σ for constant velocity crack propagation ($v=0.4C_s$) in the model of Figure 1.

Figure 5. Nondimensionalized K_I vs Σ for constant velocity crack propagation ($v=0.6C_s$) in the model of Figure 1.

Figure 6. K_{ID} vs $\hat{\Sigma}$ used as the crack growth criterion for the application (propagation) phase calculation of Figure 7.

Figure 7. Application phase analysis of the double cantilever beam specimen (No. 4) of Kalthoff et al [6].

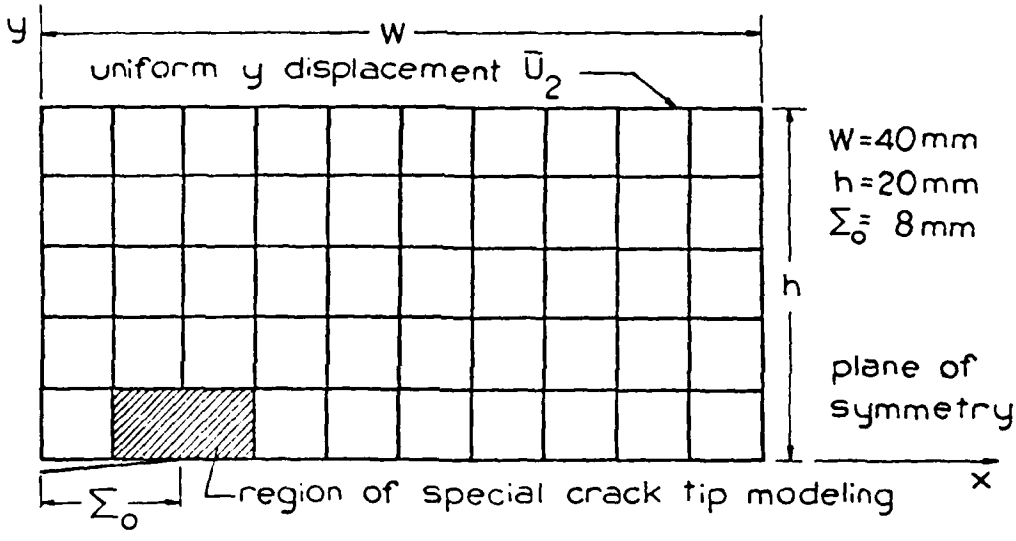

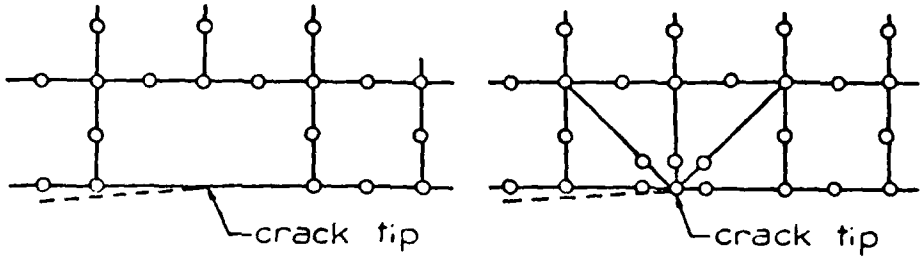

Special Element

Degenerate 8-Node Isoparametric Elements

TYPE A: Moving singular element

TYPE B: Distorting regular element

TYPE C: Non-Distorting regular element

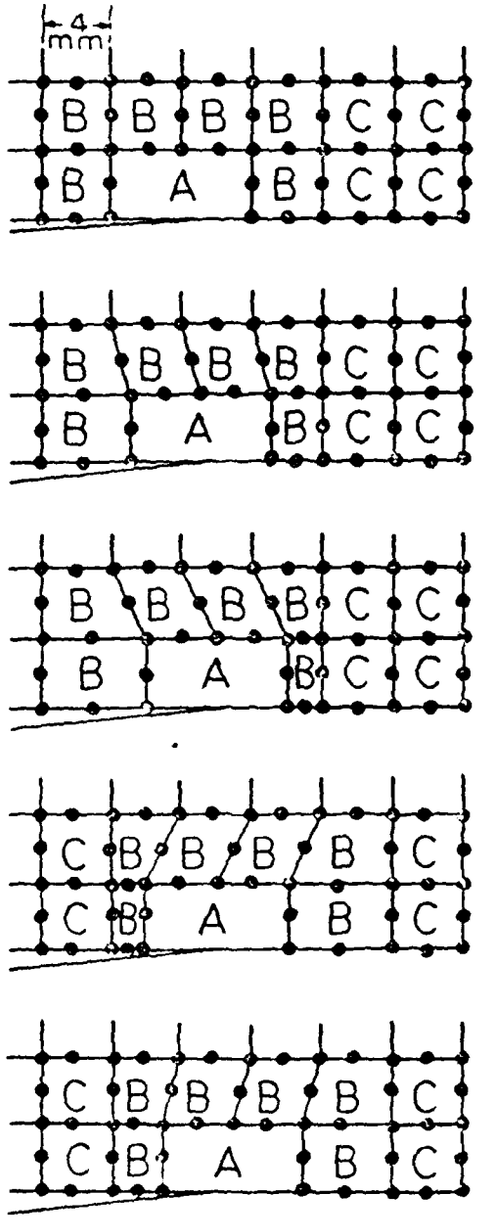

EXAMPLE : $v = 1000$ m/sec

$\Delta t = 0.2$ μsec

$\Delta \Sigma = 0.2$ mm

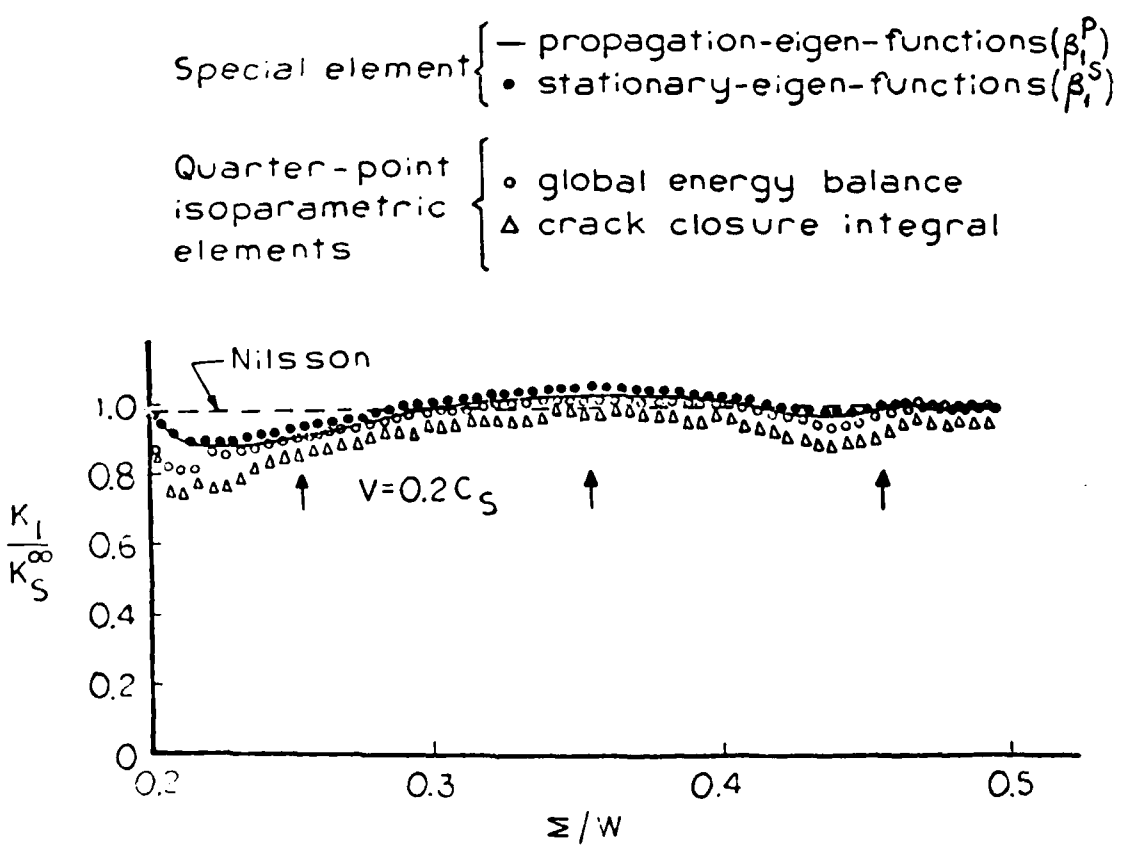
Special element
— propagation-eigen-functions(β_1^P)
• stationary-eigen-functions(β_1^S)
Quarter-point isoparametric elements
∘ global energy balance
Δ crack closure integral
Nilsson
V=0.2 C_S
$\frac{K_I}{K_S^\infty}$
1.0
0.8
0.6
0.4
0.2
0
0.2
0.3
0.4
0.5
a / W

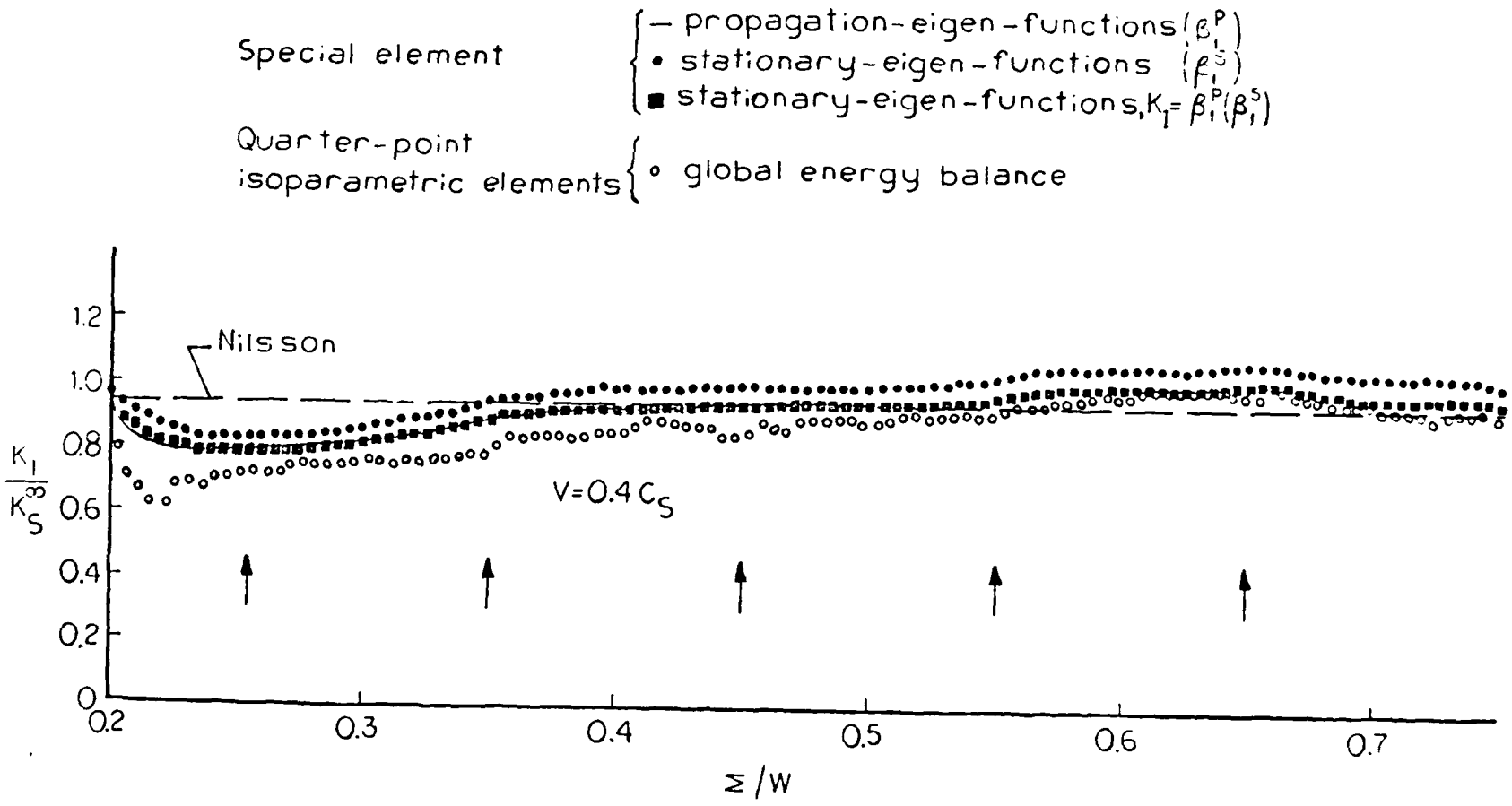
Special element
— propagation-eigen-functions (β_1^P)
• stationary-eigen-functions (β_1^S)
■ stationary-eigen-functions, $K_1 = \beta_1^P(\beta_1^S)$
Quarter-point isoparametric elements
∘ global energy balance
Nilsson
V=0.4 C_S
$\frac{K_1}{K_S^\infty}$
1.2
1.0
0.8
0.6
0.4
0.2
0
0.2
0.3
0.4
0.5
0.6
0.7
Σ/W

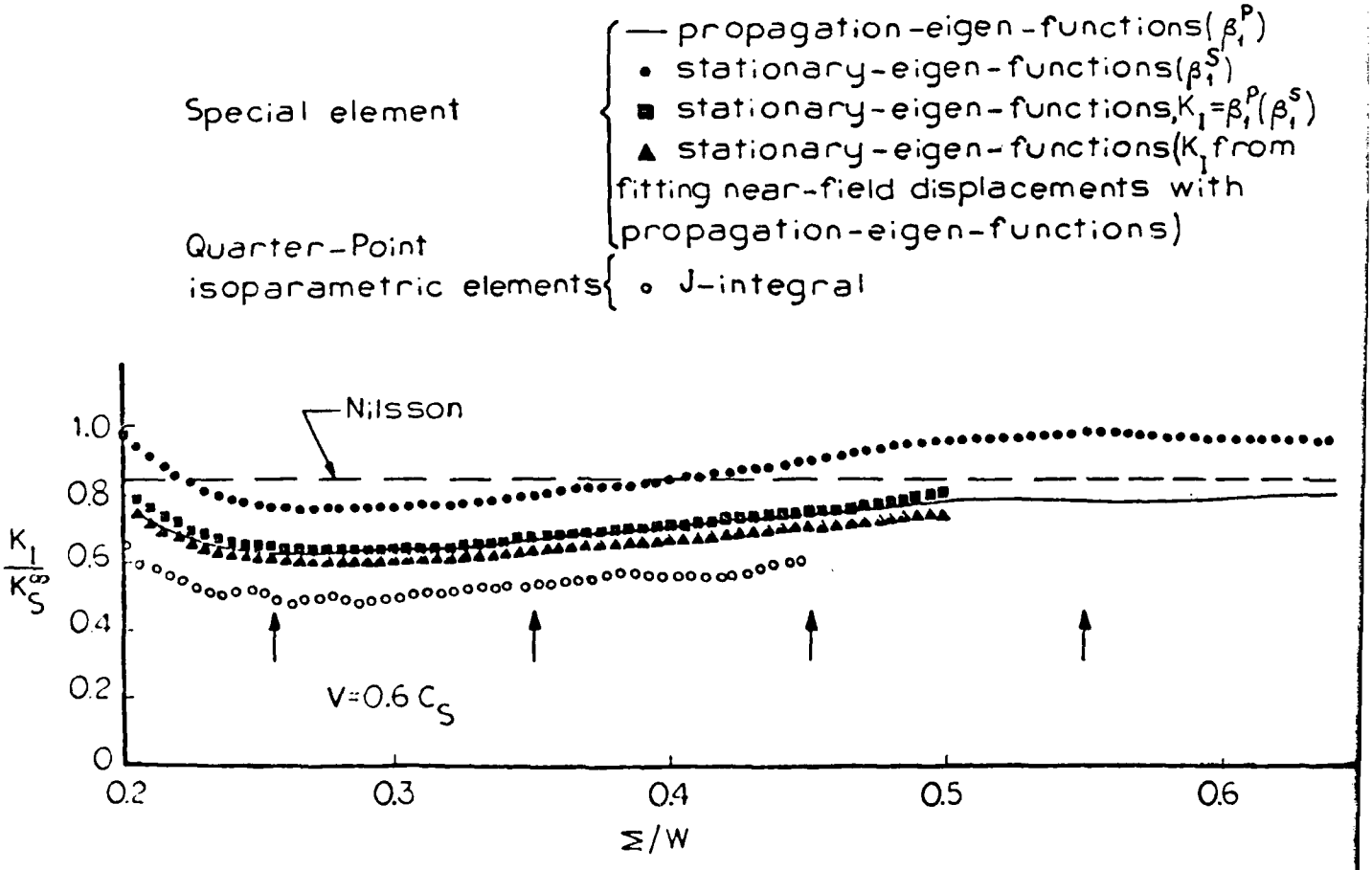
Special element
— propagation-eigen-functions(β_1^P)
• stationary-eigen-functions(β_1^S)
■ stationary-eigen-functions, $K_I=\beta_1^P(\beta_1^S)$
▲ stationary-eigen-functions(K_I from fitting near-field displacements with propagation-eigen-functions)
Quarter-Point isoparametric elements
∘ J-integral
Nilsson
$\frac{K_I}{K_S^\infty}$
1.0
0.8
0.6
0.4
0.2
0
V=0.6 C_S
0.2
0.3
0.4
0.5
0.6
Σ/W

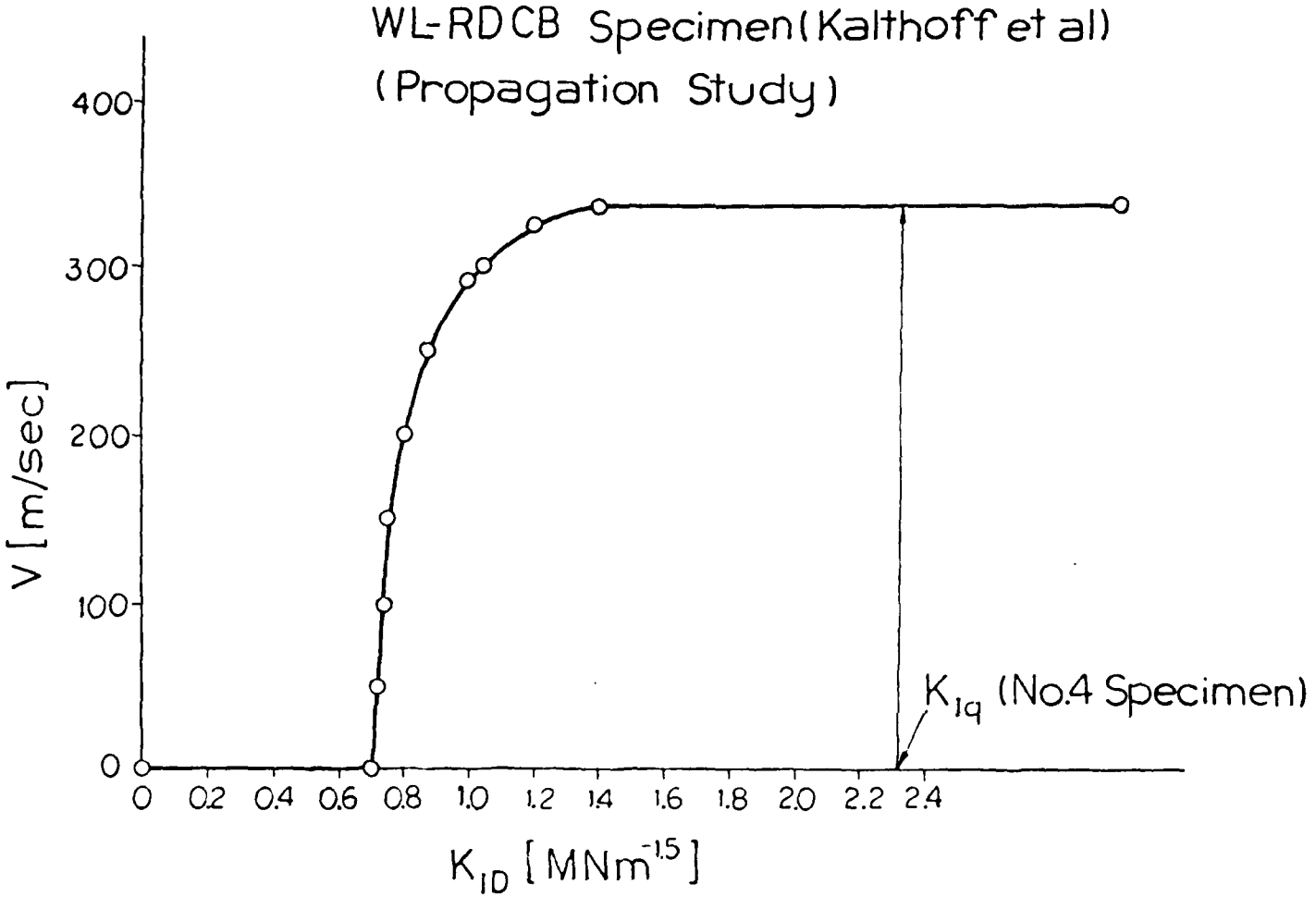
WL-RDCB Specimen(Kalthoff et al)
(Propagation Study)
400
300
200
100
0
V [m/sec]
0 0.2 0.4 0.6 0.8 1.0 1.2 1.4 1.6 1.8 2.0 2.2 2.4
K_{ID} [$MNm^{-1.5}$]
K_{Iq} (No.4 Specimen)

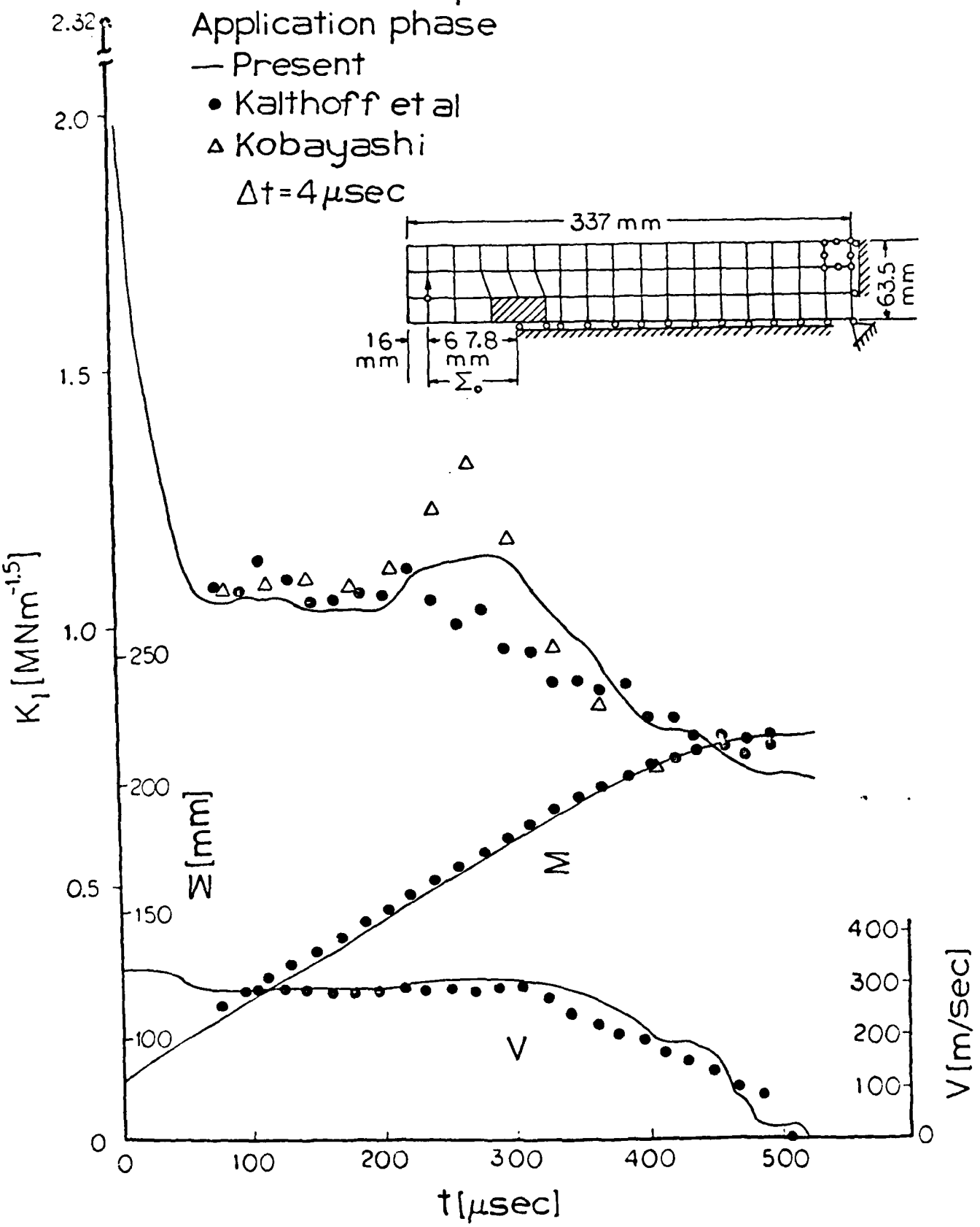
Kalthoff No.4 Specimen
Application phase
— Present
• Kalthoff et al
△ Kobayashi
Δt = 4 μsec
337 mm
63.5 mm
16 mm
6 7.8 mm
Σ₀
2.32
2.0
1.5
1.0
0.5
0
K₁ [MNm^-1.5]
250
200
150
100
W [mm]
W
V
400
300
200
100
0
V [m/sec]
0
100
200
300
400
500
t [μsec]

SECURITY CLASSIFICATION OF THIS PAGE (When Data Entered)

REPORT DOCUMENTATION PAGE

READ INSTRUCTIONS BEFORE COMPLETING FORM

1 REPORT NUMBER: 81-GIT-CACM-SNA-13	2 GOVT ACCESSION NO: AD-A103075
3 RECIPIENT'S CATALOG NUMBER:	
4 TITLE (and Subtitle): An Evaluation of Several Moving Singularity Finite Element Models for Fast Fracture Analysis	5 TYPE OF REPORT & PERIOD COVERED: Interim Report
	6 PERFORMING ORG. REPORT NUMBER: ~~81-~~GIT-CACM-SNA-13
7 AUTHOR(s): T. Nishioka, R.B. Stonesifer, S.N. Atluri	8 CONTRACT OR GRANT NUMBER(s): N00014-78-C-0636
9 PERFORMING ORGANIZATION NAME AND ADDRESS: GIT - Center for the Advancement of Computational Mechanics, School of Civil Engineering Atlanta, GA 30332	10 PROGRAM ELEMENT, PROJECT, TASK AREA & WORK UNIT NUMBERS: NE064-610
11 CONTROLLING OFFICE NAME AND ADDRESS: Office of Naval Research Structural Mechanics Program Dept. of Navy, Arlington, VA 22217	12 REPORT DATE: July 1981
	13 NUMBER OF PAGES: 34
14 MONITORING AGENCY NAME & ADDRESS (if different from Controlling Office)	15 SECURITY CLASS (of this report): Unclassified
	15a DECLASSIFICATION/DOWNGRADING SCHEDULE:

16 DISTRIBUTION STATEMENT (of this Report)

Unlimited

[illegible] Approved for public release and sale; its distribution is unlimited.

17 DISTRIBUTION STATEMENT (of the abstract entered in Block 20, if different from Report)

18 SUPPLEMENTARY NOTES

19 KEY WORDS (Continue on reverse side if necessary and identify by block number)

20 ABSTRACT (Continue on reverse side if necessary and identify by block number)

DD FORM 1 JAN 73 1473 EDITION OF 1 NOV 65 IS OBSOLETE

SECURITY CLASSIFICATION OF THIS PAGE (When Data Entered)

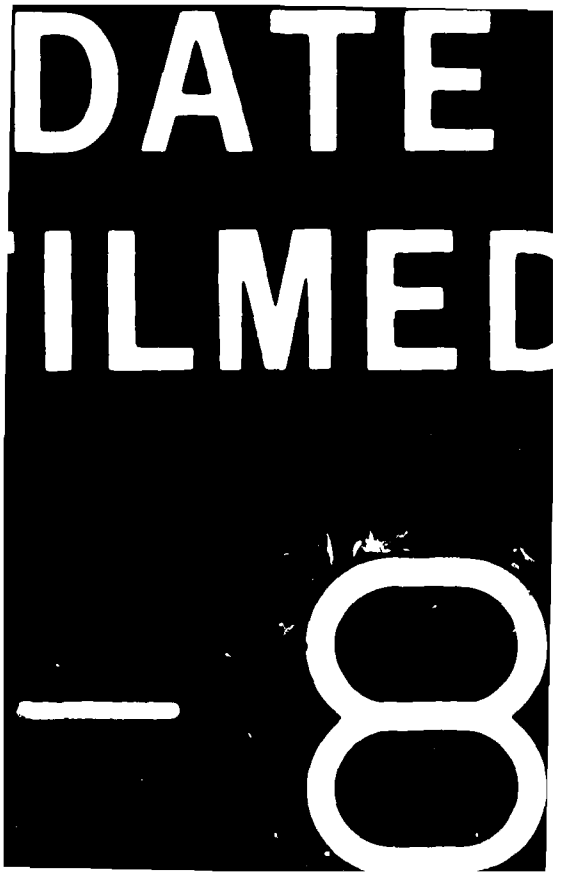
DATE
ILMED
8